Spatio-temporal measurements of the electronic density in a diffuse corona discharge under extreme voltage conditions

A. Brisset[1], A. Sobota[2], P. Tardiveau[1]

[1]Laboratoire de Physique des Gaz et des Plasmas, Paris-Saclay University, Orsay, France
[2]Department of Applied Physics, Eindhoven University of Technology, Eindhoven, The Netherlands

Abstract: The spatio-temporal electron density and temperature of a non-thermal diffuse discharge in a pin-to-plane atmospheric air gap is measured with incoherent Thomson scattering technic. The discharge is generated by a 10 ns and 85 kV voltage pulse run at 10 Hz. Electron densities of the order of 10^{21} m^{-3} are reached on the axis and spread radially over 2 to 4 mm. Those densities are two orders of magnitude higher than other similar non-thermal discharges.

Keywords: Thomson scattering, nanosecond discharge, diffuse atmospheric plasma, streamer

1. Introduction

The generation of non-thermal and largely diffuse discharges in centimetre atmospheric air gaps is obtained by applying pulsed extreme overvoltages [1]. It is a quite new and different kind of discharge compared to the well-known streamer regime obtained at moderate overvoltage. The streamer-to-diffuse transition is characterized by strong modifications of some of the discharge properties such as the spatial extension of the electric field distribution during both the propagation and conduction phase [2]. The spatio-temporal determination of the electron density is also targeted to describe this transition. When coupled to the electric field distribution, it becomes very helpful to determine the electrical power density transferred into the gas. Beside the challenging physics which appears at high overvoltage, the power density combined with the extended volume of the discharge are of great interest for various applications, specifically flow control or gas treatment [3].

Incoherent Thomson scattering (ITS) is a non-invasive and spatially-resolved complex diagnostic applied for electron density and temperature measurements [4,5]. It is based on the scattering interaction of a laser photon with a charged particle of the plasma, specifically free electrons. The ITS signal is a broad, low intensity signal spectrally confined next to the laser wavelength. Therefore, it is highly disturbed by the Rayleigh emission and in the case of a molecular gas by the rotational Raman emission lines as well, due to the inelastic interaction of the laser with the molecules. The Rayleigh scattering can be removed either by a highly dispersive spectrometer (triple-grating spectrometer) or by a high quality Notch or Bragg filter. The ITS signal is then determined by the fitting of experimental and theoretical spectra of both ITS and Raman emissions.

In the case of atmospheric pressure air discharges, for low electron densities or high electron temperatures, the intensity ratio between the ITS and Raman emission may be too low to allow accurate measurements of the ITS signal [5,6]. For this reason, the ITS diagnostic has rarely been applied for very transient air streamers and is still under development [7]. When it is possible, electrostatic probes or optical emission spectroscopic methods based on the Stark broadening of emission lines are being preferred. In atmospheric air, however, the Van der Waals broadening is often too large compared to the Stark broadening to implement this method for electronic densities below 10^{17} cm^{-3} [8,9]. The stable and volumetric discharge under study allows for averaged measurements. Moreover, a rough estimation of the electron density determined from discharge current measurements under the extreme voltage conditions suggest that electron densities of the order of 10^{15} cm^{-3} can be expected. ITS measurements were therefore implemented despite the remaining challenges.

The main goals of the present study are to evaluate how extreme voltage pulses affect the electron density and temperature of the discharge in space and time and to relate these measurements to the specificities of the discharge development.

2. Experimental set up

The diffuse discharge device is fully described in [1]. It is generated in atmospheric air in a pin-to-plane geometry across an 18 mm gap. The pin is made of tungsten with 100 µm curvature radius and the grounded copper plane is 5 cm radius. The nanosecond pulse supplied with a FID-type generator is delivered to the pin. Typical electrical signals at 85 kV peak voltage are presented in Fig. *1*, with voltage rise time of 2 ns and full width high maximum of 5 ns. It is run at 10 Hz to limit memory effects.

The experimental setup is presented in Fig. *2*. A 532 nm laser of 200 ps pulse duration is used. In order to avoid laser induced breakdown events, the beam energy is limited to 70 mJ. A plano-convex lens of 1 m focal length focuses the beam on the discharge, in this configuration the Rayleigh range is 0.7 cm and the minimum beam width is 68 µm. The scattered Thomson signal is collected at 90° from the laser path and perpendicularly to the laser polarisation.It is focused into a triple-grating spectrometer with a collimator made of two 10 cm diameter lenses. A first slit collects the light along the 1D horizontal radial axis. It is followed by an image rotator and a first grating then disperses the light. It is focused by a lens on a mask to remove the large majority of the Rayleigh scattered light. Then, the remaining Thomson and rotational Raman signals are re-collected by a second grating which reconstructs the initial image at the first slit except the Rayleigh signal is removed. The rest of the triple-grating spectrometer acts as a normal spectrometer: the second entrance slit (80 µm) sets the spectral resolution (0.08 nm) (and removes the remaining stray light) along with the third grating (1200 g.m^{-1}) which disperses light before it is collected by an Andor ICCD camera.

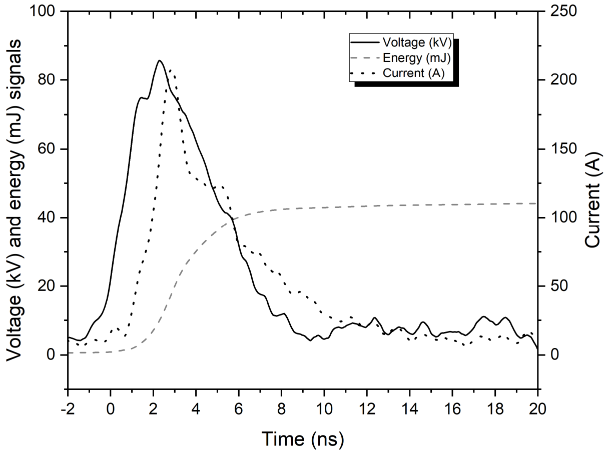

Fig. 1. Voltage, current and energy signals for a typical 85kV peak voltage pulse.

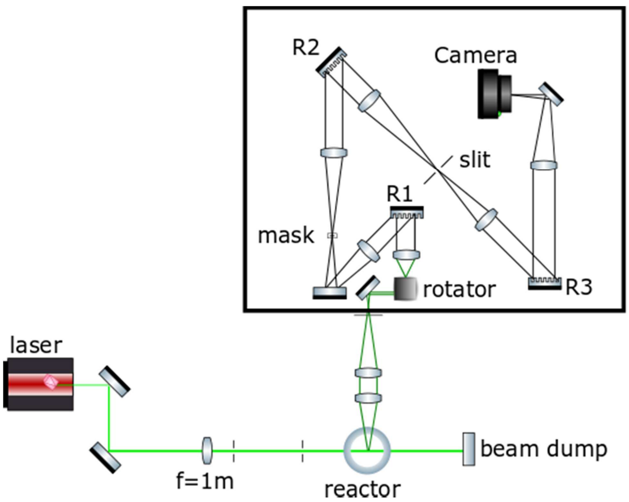

Fig. 2. Experimental set up of Thomson scattering.

3. Synchronization and data reduction

During the operation, the discharge and the laser flash lamps are triggered by an external master clock at 10 Hz. In order to achieve time resolution better than 500 ps and to be independent from the internal time jitter of the power supply, the Q-switch of the laser is triggered separately with the output synchronisation TTL signal of the generator. This signal is delivered precisely 256 ns before the high voltage pulse. The camera of the spectrometer having a short time response is also triggered by the output synchronisation signal. This way, the time resolution is determined by the laser 500 ps jitter.

In atmospheric air, the collected signal is made up of three different signals: the Thomson scattered signal which is spectrally broad and which intensity is maximum around the laser wavelength in case of ITS, the rotational Raman scattering which is a combination of nitrogen and oxygen emission lines highly dependent on the instrumental function of the spectrometer and the Rayleigh signal which is efficiently removed by the triple grating spectrometer.

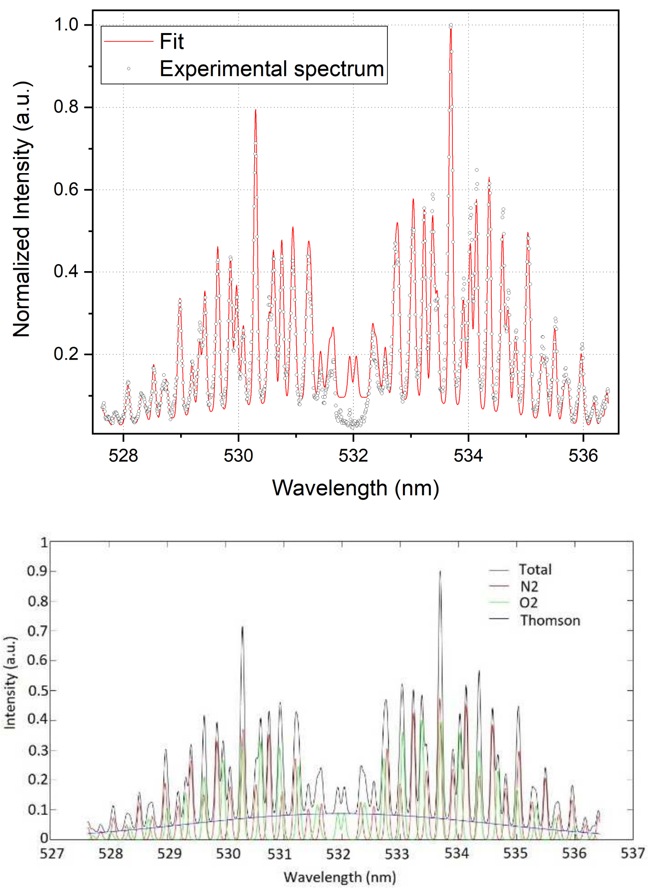

Fig. 3. a) Experimental scattering measurement and fit at 85 kV at 1.3 mm from the pin on the axis. The spectrum is averaged over 30 000 shots and 50 radial pixel binning corresponding to 1 mm. b) The different signals of the fit of a) are deconvoluted to highlight their respective contributions.

Since the Raman lines cover the whole spectrum range of Thomson occurrence and since they are not isolated, the Thomson signal cannot be determined through a baseline and the Raman spectrum has to be very accurately determined. The Thomson signal is analysed by fitting theoretical and experimental spectra. The Matlab-based algorithm used is described in [10,11]. The uncertainties of the fitted parameters are determined by the Matlab function *nlparci* as 95 % confidence interval of the least squared method. An example of time-resolved spectrum at 85 kV and 1.3 mm from the pin is presented in Fig. *3*.

4. Results

An order of magnitude of the electron density can be estimated from current measurements in the conduction phase of the discharge. In a first approximation, the average field along the axis in the plasma channel can be determined by dividing the applied voltage by the gap width. For field range between 10 and 50 kV.cm^{-1}, the electron density is between 10^{20} and 10^{21} m^{-3}.

First spatio-temporal measurements obtained by ITS are presented in

Fig. *4*. Electron density up to 1.6*10^{21} m^{-3} are obtained during the conduction phase of the discharge at 1.3 mm from the pin, for electron temperatures around 4 eV. The radial extent of the electron density is about 2 mm at FWHM. This is well in the range of the current-based estimation. Such values are similar to other short-pulsed atmospheric discharges in air: values of 10^{20} – 10^{21} m^{-3} have been measured for nanosecond repetitively pulse glows [12]. It is much higher compared to plasma jets: electron densities of a pulsed He jet in atmospheric air facing a metallic target remain of the order of 10^{19} m^{-3} even just above the target [11]. On the contrary, for micro-discharges, transient spark discharges or long pulsed discharges, the maximum values of 10^{23}-10^{25} m^{-3} can be obtained [8,9,13] according to conductivity measurements and Stark broadening on H, O and N.

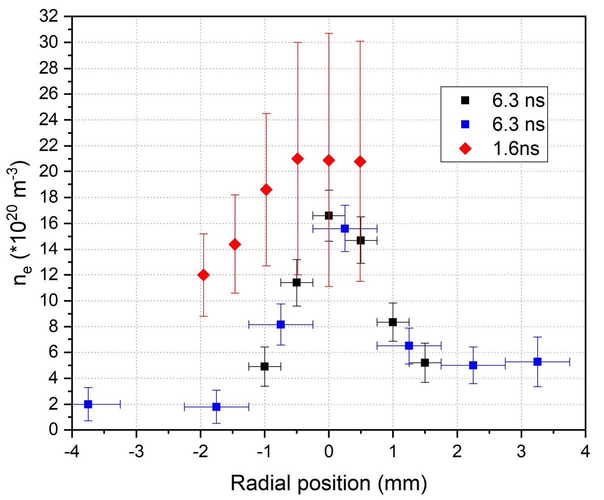

Fig. 4. Radial profile at 85 kV and 6.3 ns at 1.3 mm from the pin for two spatial resolutions (0.5 and 1 mm) and at 1.6 ns with 0.5 mm spatial resolution.

For such electron densities, the TS interaction is close to the limit between the coherent and incoherent scattering regimes. The scattering regime is governed by the coherence parameter and the limit has been approximately set to 3.10^{21} m^{-3} [14]. For each condition, the data presented in this work was analysed under the incoherent assumption.

The maximum electronic density seems to be produced in the first instants of the discharge and reaches about 2*10^{21} m^{-3} (cf. figure 4). The spatial extent of those high electron densities is more than 2 mm radius at the pin and extends to about 4 mm at 9 mm from the pin (cf. **Erreur ! Source du renvoi introuvable.**5). The uncertainty is high with low electron densities and high electron temperatures. Therefore, at 9 mm from the pin where the discharge diameter is extended over 1.5 cm, the electrons are probably distributed over a volume so large that the electron density is too low to be measured as plotted in figure 5.

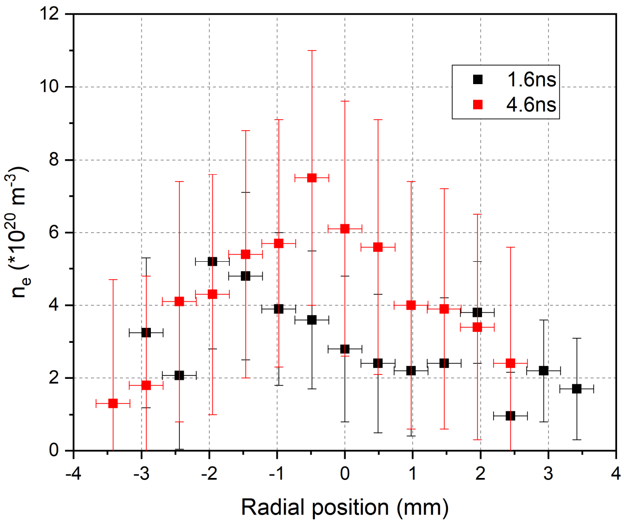

Fig. 5. Radial profiles at 85 kV and 1.6 and 4.6 ns at 9 mm from the pin.

5. Conclusion

The electron properties of a nanosecond diffuse corona discharge under extreme overvoltages are studied by incoherent Thomson scattering. A triple grating spectrometer is used to cut off the Rayleigh and stray light emission. Electron densities reach a few 10^{21} m^{-3} on the axis and spread radially over 2 to 4 mm. Such densities are similar to classical lower voltage streamers except they are distributed over a much larger volume. Uncertainties can be high (~50%) due to high electron temperatures since the signal-to-noise ratio of Thomson and Raman emissions is low in these conditions.

6. Acknowledgment

This work is supported by the Agence Nationale de la Recherche in the frame of the ANR-13-BS09-0014 research program.

7. References

[1] Tardiveau P, Magne L, Marode E, Ouaras K, Jeanney P and Bournonville B, Plasma Sources Sci. Technol. **25** 054005 (2016)

[2] Brisset A, Gazeli K, Magne L, Pasquiers S, Jeanney P, Marode E and Tardiveau P, Plasma Sources Sci. and Technol. Submitted (2018)

[3] Ouaras K, Magne L, Pasquiers S, Tardiveau P, Jeanney P and Bournonville B, Plasma Sources Sci. Technol. **27** 045002 (2018)

[4] Carbone E and Nijdam S, Plasma Phys. Control. Fusion **57** 014026 (2015)

[5] Hübner S, Sousa J S, Mullen J van der and Graham W G, Plasma Sources Sci. Technol. **24** 054005 (2015)

[6] Gessel A F H van, Carbone E A D, Bruggeman P J and Mullen J J A M van der, Plasma Sources Sci. Technol. **21** 015003 (2012)

[7] Vincent B, Tsikata S, Mazouffre S, Minea T and Fils J, Plasma Sources Sci. Technol. **27** 055002 (2018)

[8] Orrière T, Moreau E and Pai D Z, J. Phys. D: Appl. Phys. **51** 494002 (2018)

[9] Janda M, Martišovitš V, Hensel K, Dvonč L and Machala Z, Plasma Sources Sci. Technol. **23** 065016 (2014)

[10] Klarenaar B L M, Grofulović M, Morillo-Candas A S, Bekerom D C M van den, Damen M A, Sanden M C M van de, Guaitella O and Engeln R, Plasma Sources Sci. Technol. **27** 045009 (2018)

[11] Klarenaar B L M, Guaitella O, Engeln R and Sobota A, Plasma Sources Sci. Technol. **27** 085004 (2018)

[12] Rusterholtz D L, Lacoste D A, Stancu G D, Pai D Z and Laux C O, J. Phys. D: Appl. Phys. **46** 464010 (2013)

[13] Lo A, Cessou A, Lacour C, Lecordier B, Boubert P, Xu D A, Laux C O and Vervisch P, Plasma Sources Sci. Technol. **26** 045012 (2017)

[14] Warner K and Hieftje G M, Spectrochimica Acta **57** 201–41 (2002)